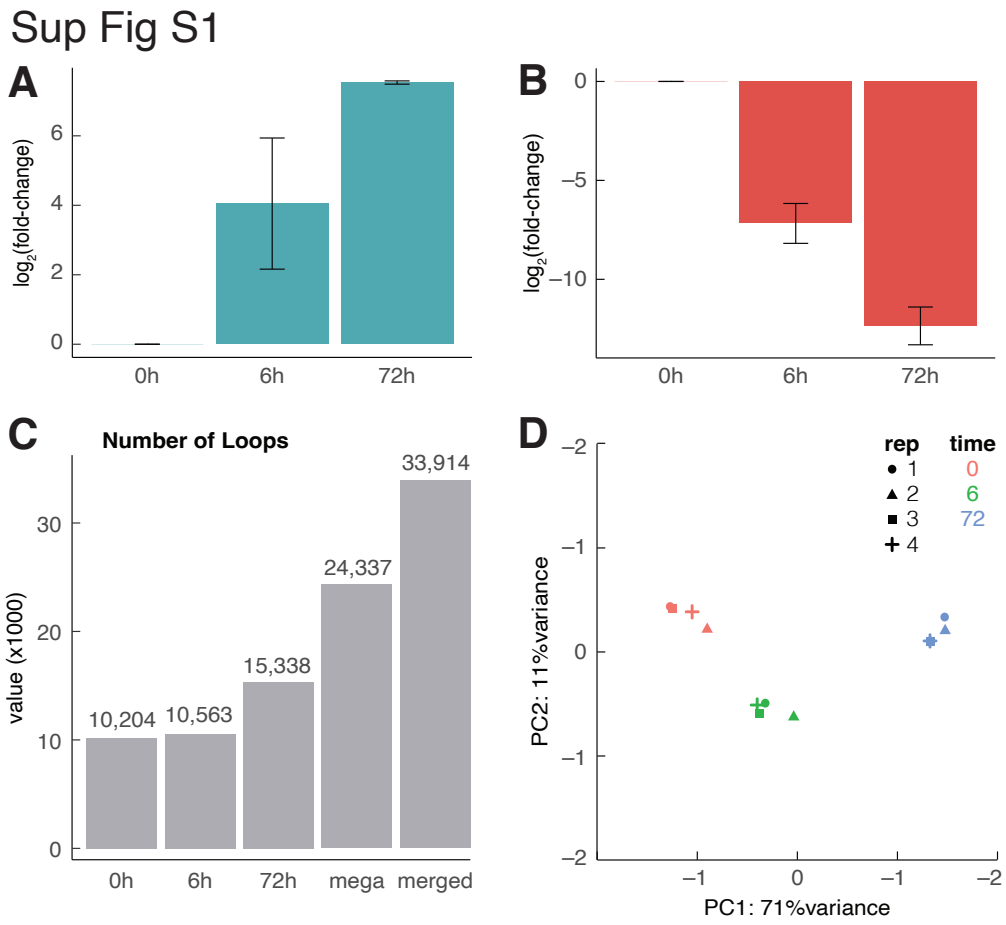

Figure S1. Confirmation of megakaryocyte differentiation and detection of loops. qPCR analysis of **(A)** *ITGB3* and **(B)** *KLF1* over megakaryocyte differentiation at 0, 6, and 72h. Two biological replicates and 4 technical replicates were collected, normalized to *GAPDH* levels, and $\log_2$(fold-change) was calculated relative to 0h. **(C)** Number of loops identified with SIP after 0, 6, or 72h of differentiation, after merging all timepoints together into the Mega map, and merging all timepoints together with mariner. **(D)** PCA plot showing similarities in loop counts between replicates and timepoints.

Sup Fig S2

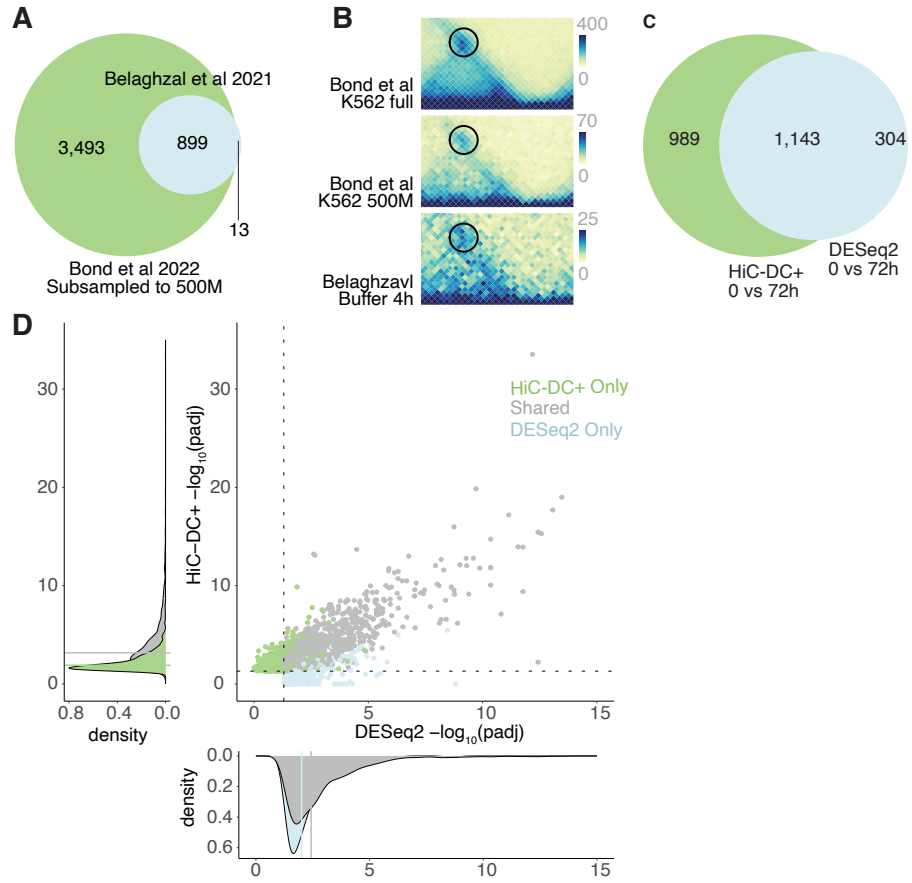

Figure S2. Loops are similar to previous studies and other differential looping strategies. **(A)** Venn diagram comparing loops from K562s in this study subsampled to 500 million reads to loops from Belaghzal et al 2021. **(B)** Representative loop for full K562 data from this study (top) the data subsampled to 500M reads (middle), and Belaghzal et al (bottom). **(C)** Venn diagram comparing the differential loops identified in this study by DESeq2 (0 vs 72h) and differential loops identified from HiC-DC+ (0 vs 72h). **(D)** Scatter plot comparing adjusted p-values for DESeq2 (0 vs 72h) to adjusted p-values for HiC-DC+ (0 vs 72h). The y-axis includes a density plot showing the differences in distributions of the HiC-DC+ specific differential loops to the shared differential loops between both loop callers. The x-axis includes a density plot showing the differences in distributions of the DESeq2 specific differential loops to the shared differential loops between both loop callers. Gray lines on the density plots represent the median of the shared loop distribution (3.16 on the y-axis and 2.42 on the x-axis), green line represents the median of the HiC-DC+ only distribution (1.9), blue line represents the median of the DESeq2 only distribution (2.01).

Sup Fig S3

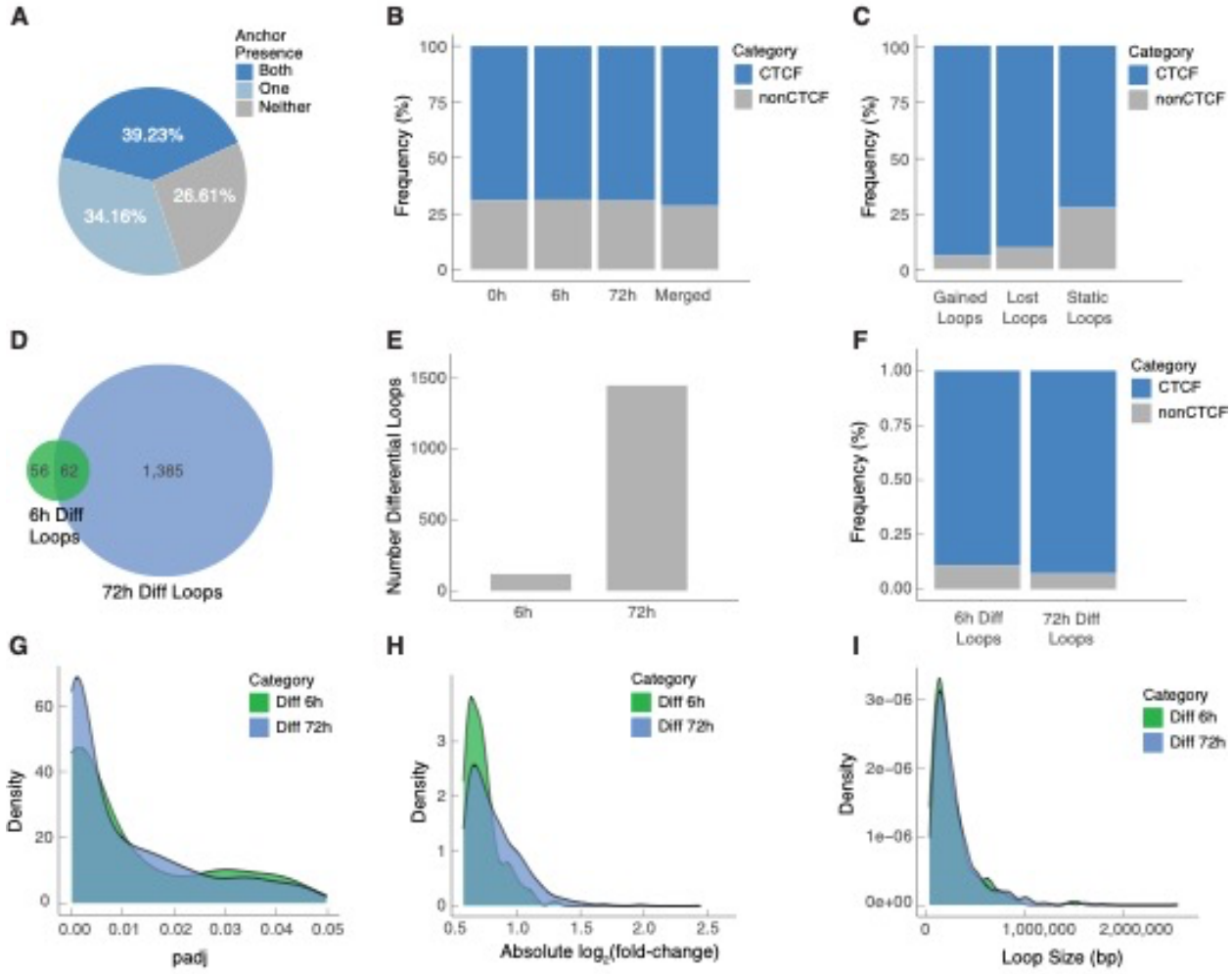

Figure S3. CTCF is bound at a majority of loops and there are minimal differences between differential loops after 6h and 72h. (A) Pie chart showing percentage of loops that have CTCF at both anchors, one anchor, or neither anchor. **(B)** Proportion of CTCF and non-CTCF bound loops at each time point, and the merged map. **(C)** Proportion of CTCF and non-CTCF bound loops for gained, lost, and static loops. **(D)** Venn diagram comparing differential loops at 6h and 72h. **(E)** Number of differential loops identified at 6h and 72h. **(F)** Proportion of CTCF and non-CTCF bound loops for differential loops at 6h and 72h. **(G)** Distribution of adjusted p values for differential loops at 6h and 72h. **(H)** Distribution of log_2(fold-changes) for differential loops at 6h and 72h. **(I)** Distribution of loop sizes for differential loops at 6h and 72h.

Sup Fig S4

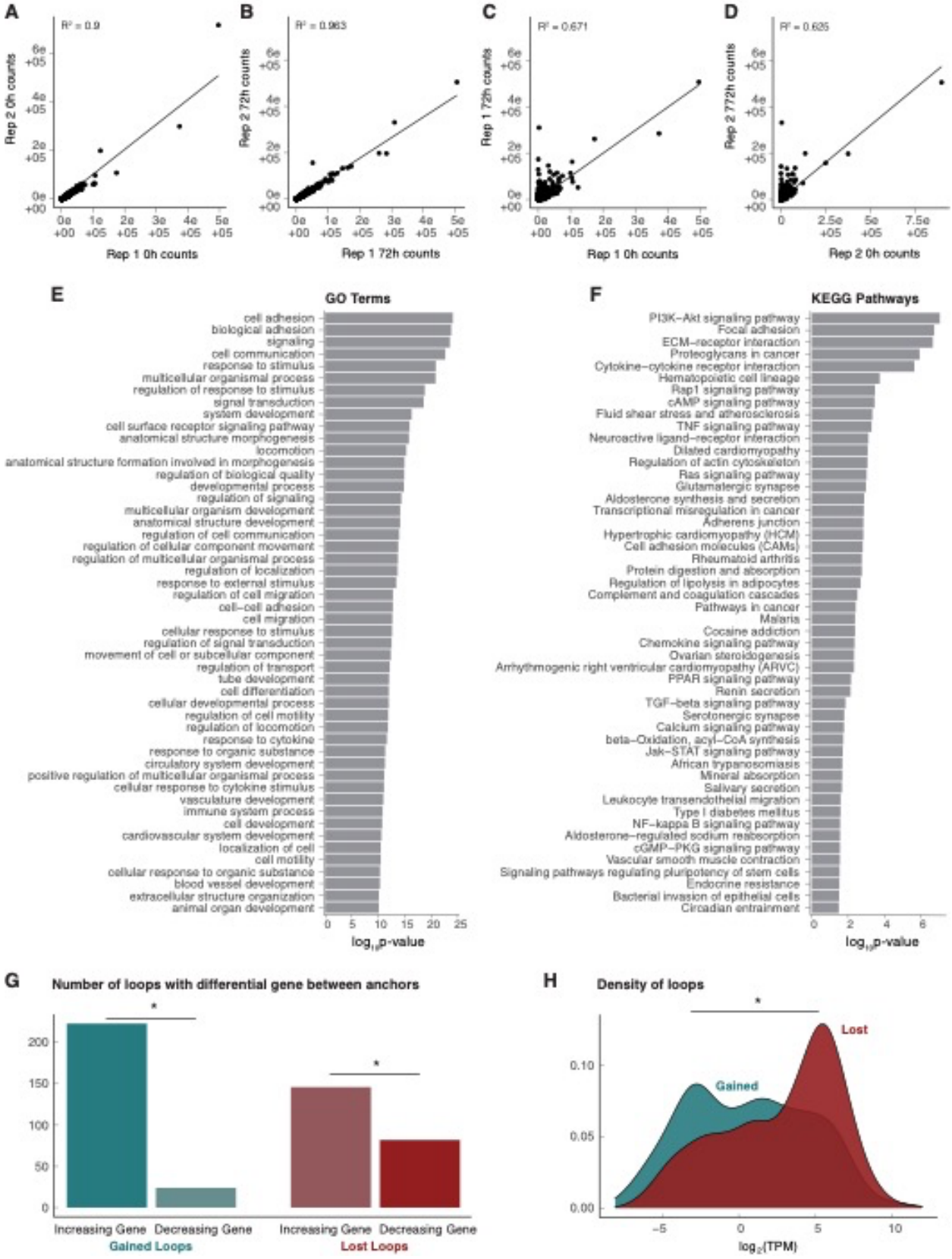
A
R² = 0.9
Rep 2 0h counts
Rep 1 0h counts
B
R² = 0.983
Rep 2 72h counts
Rep 1 72h counts
C
R² = 0.671
Rep 1 72h counts
Rep 1 0h counts
D
R² = 0.625
Rep 2 72h counts
Rep 2 0h counts
E
GO Terms
cell adhesion
biological adhesion
signaling
cell communication
response to stimulus
multicellular organismal process
regulation of response to stimulus
signal transduction
system development
cell surface receptor signaling pathway
anatomical structure morphogenesis
locomotion
anatomical structure formation involved in morphogenesis
regulation of biological quality
developmental process
regulation of signaling
multicellular organism development
anatomical structure development
regulation of cell communication
regulation of cellular component movement
regulation of multicellular organismal process
regulation of localization
response to external stimulus
regulation of cell migration
cell–cell adhesion
cell migration
cellular response to stimulus
regulation of signal transduction
movement of cell or subcellular component
regulation of transport
tube development
cell differentiation
cellular developmental process
regulation of cell motility
regulation of locomotion
response to cytokine
response to organic substance
circulatory system development
positive regulation of multicellular organismal process
cellular response to cytokine stimulus
vasculature development
immune system process
cell development
cardiovascular system development
localization of cell
cell motility
cellular response to organic substance
blood vessel development
extracellular structure organization
animal organ development
log10p-value
F
KEGG Pathways
PI3K–Akt signaling pathway
Focal adhesion
ECM–receptor interaction
Proteoglycans in cancer
Cytokine–cytokine receptor interaction
Hematopoietic cell lineage
Rap1 signaling pathway
cAMP signaling pathway
Fluid shear stress and atherosclerosis
TNF signaling pathway
Neuroactive ligand–receptor interaction
Dilated cardiomyopathy
Regulation of actin cytoskeleton
Ras signaling pathway
Glutamatergic synapse
Aldosterone synthesis and secretion
Transcriptional misregulation in cancer
Adherens junction
Hypertrophic cardiomyopathy (HCM)
Cell adhesion molecules (CAMs)
Rheumatoid arthritis
Protein digestion and absorption
Regulation of lipolysis in adipocytes
Complement and coagulation cascades
Pathways in cancer
Malaria
Cocaine addiction
Chemokine signaling pathway
Ovarian steroidogenesis
Arrhythmogenic right ventricular cardiomyopathy (ARVC)
PPAR signaling pathway
Renin secretion
TGF–beta signaling pathway
Serotonergic synapse
Calcium signaling pathway
beta–Oxidation, acyl–CoA synthesis
Jak–STAT signaling pathway
African trypanosomiasis
Mineral absorption
Salivary secretion
Leukocyte transendothelial migration
Type I diabetes mellitus
NF–kappa B signaling pathway
Aldosterone–regulated sodium reabsorption
cGMP–PKG signaling pathway
Vascular smooth muscle contraction
Signaling pathways regulating pluripotency of stem cells
Endocrine resistance
Bacterial invasion of epithelial cells
Circadian entrainment
Circadian entrainment
log10p-value
G
Number of loops with differential gene between anchors
Increasing Gene
Decreasing Gene
Gained Loops
Increasing Gene
Decreasing Gene
Lost Loops
H
Density of loops
Lost
Gained
log2(TPM)

Figure S4. Replicate correlations, megakaryocyte pathway enrichment, and interior gene expression. Scatterplots showing the correlation between gene counts from **(A)** Rep 1 0h and Rep 2 0h, **(B)** Rep 1 72h and Rep 2 72h, **(C)** Rep 1 0h and Rep 1 72h, and **(D)** Rep 2 0h and Rep 2 72h (fourth). **(E)** Top 50 GO terms for up-regulated genes from RNA-seq. **(F)** Top 50 KEGG Pathways for up-regulated genes from RNA-seq. **(G)** Concordance analysis for the 475 differential loops that had a differential gene promoter between their anchors. Binomial test performed for each comparison, asterisks represent $p < 0.05$. **(H)** Expression of genes located between the anchors of gained and lost loops, asterisk represents $p < 0.05$ (TPM: transcripts per million).

Sup Fig S5

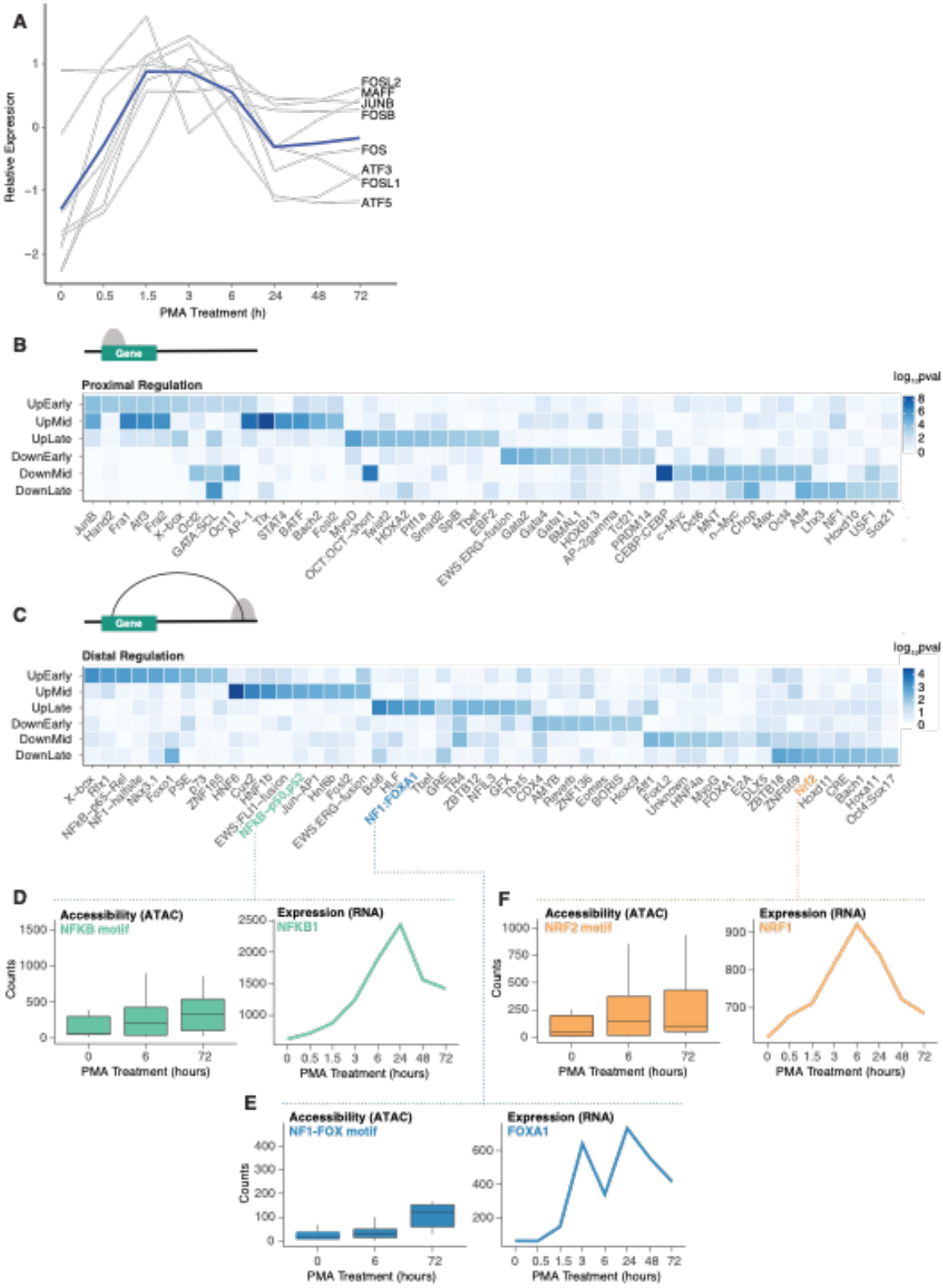
A
Relative Expression
PMA Treatment (h)
FOSL2
MAFF
JUNB
FOSB
FOS
ATF3
FOSL1
ATF5
B
Gene
Proximal Regulation
log10pval
UpEarly
UpMid
UpLate
DownEarly
DownMid
DownLate
C
Gene
Distal Regulation
log10pval
NF1:FOXA1
NFKB-p50:p65
NRF2
D
Accessibility (ATAC)
NFKB motif
Counts
PMA Treatment (hours)
Expression (RNA)
NFKB1
PMA Treatment (hours)
E
Accessibility (ATAC)
NF1-FOX motif
Counts
PMA Treatment (hours)
Expression (RNA)
FOXA1
PMA Treatment (hours)
F
Accessibility (ATAC)
NRF2 motif
Counts
PMA Treatment (hours)
Expression (RNA)
NRF1
PMA Treatment (hours)

Figure S5. AP-1 members are expressed and different sets of transcription factors are enriched at proximal and distal anchors of differential genes at loops. (A) Normalized expression of various differential expressed AP-1 family members (blue = median expression). **(B)** TFs enriched at the promoters of looped differential genes in each cluster. **(C)** TFs enriched at the distal anchors of looped differential genes in each cluster. **(D)** Chromatin accessibility of NFKB motifs over time (left) and gene expression of *NFKB1* (right). **(E)** Chromatin accessibility of NF1-FOX motif over time (left) and expression of *FOXA1* (right). **(F)** Chromatin accessibility of NRF2 motif over time (left) and expression of *NRF1* (right).

Sup Fig S6

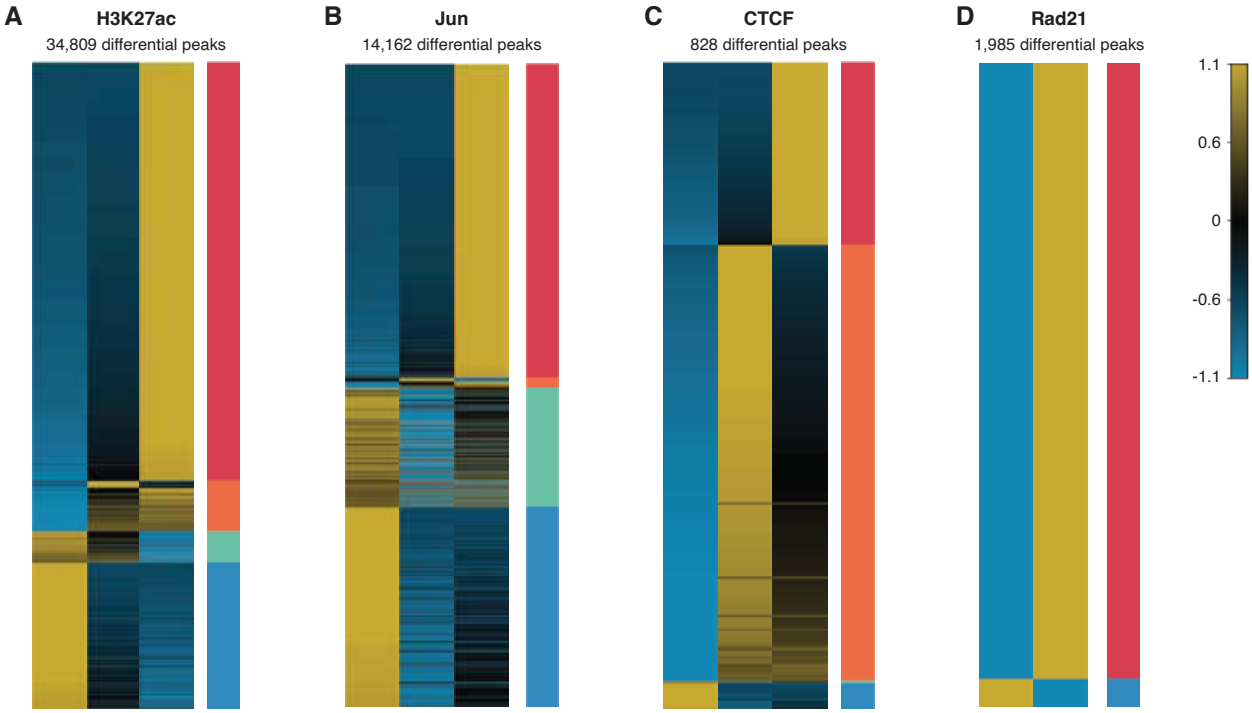

Figure S6. Differential chromatin and transcription factor binding events. Heatmaps showing normalized counts for **(A)** H3K27ac, **(B)** JUN, **(C)** CTCF, and **(D)** RAD21. Clusters are indicated by the bars on the right side of each heatmap, $p < 0.05$, $\log_2$(fold-change) > 2.

Sup Fig S7

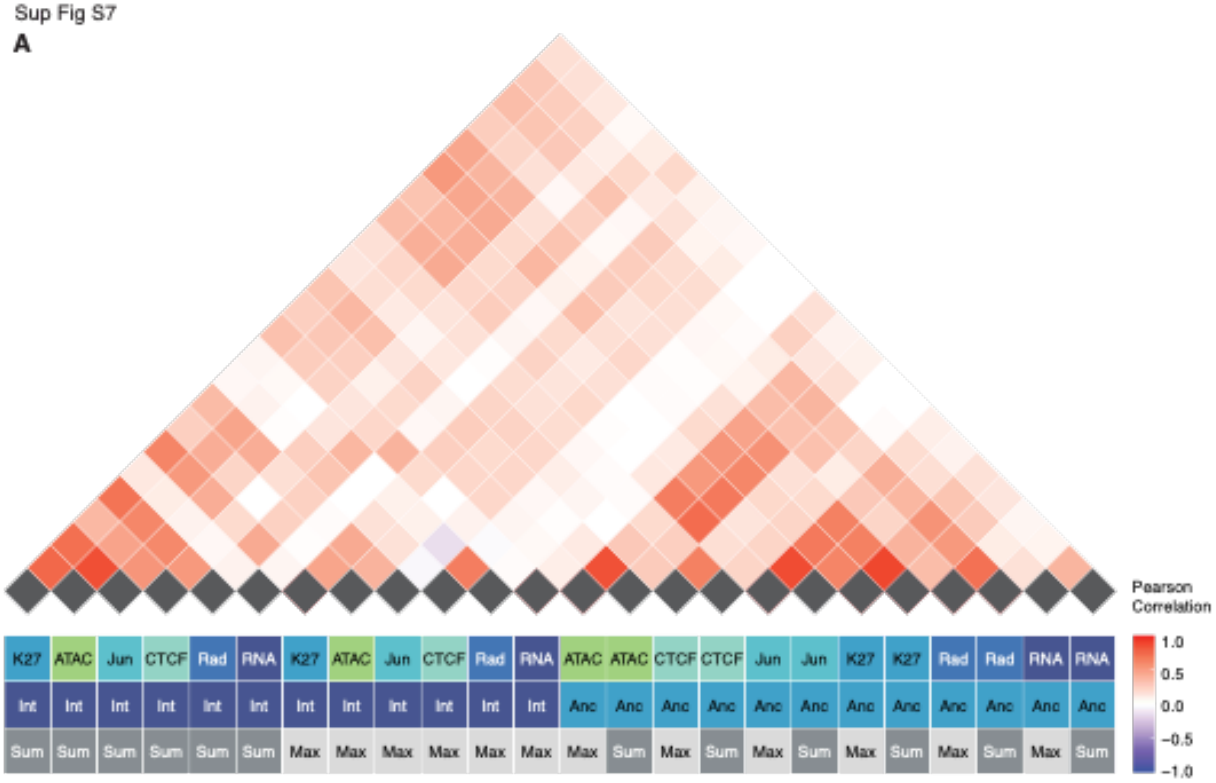
A
K27 ATAC Jun CTCF Rad RNA K27 ATAC Jun CTCF Rad RNA ATAC ATAC CTCF CTCF Jun Jun K27 K27 Rad Rad RNA RNA
Int Int Int Int Int Int Int Int Int Int Int Int Anc Anc Anc Anc Anc Anc Anc Anc Anc Anc Anc Anc
Sum Sum Sum Sum Sum Sum Max Max Max Max Max Max Max Sum Max Sum Max Sum Max Sum Max Sum Max Sum
Pearson Correlation
1.0
0.5
0.0
−0.5
−1.0

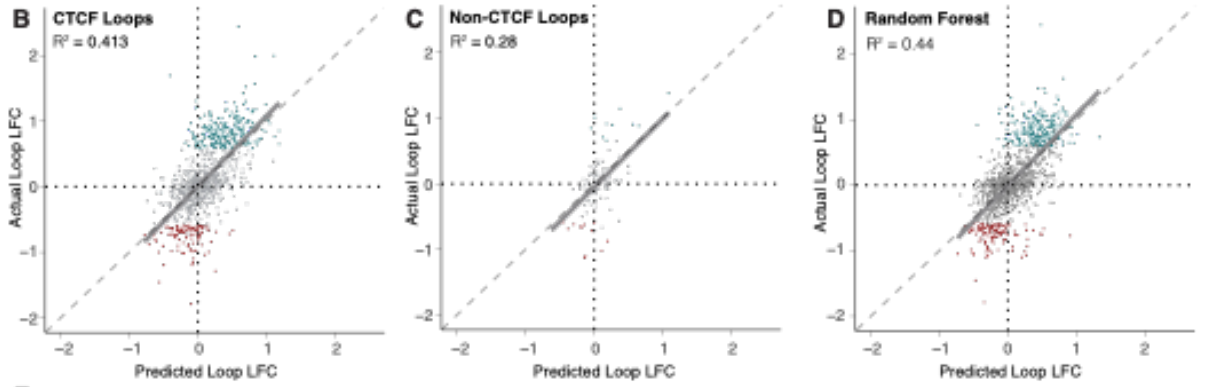
B
CTCF Loops
R² = 0.413
C
Non-CTCF Loops
R² = 0.28
D
Random Forest
R² = 0.44
Actual Loop LFC
Predicted Loop LFC


E
Absolute(Coefficient)
CTCF ATAC K27 ATAC Jun CTCF Jun Rad CTCF CTCF ATAC Jun K27 K27 RNA Rad RNA Jun Rad RNA K27 ATAC Rad RNA
Anc Int Int Anc Int Int Anc Anc Anc Int Int Int Anc Anc Int Int Int Anc Int Anc Int Anc Anc Anc
Max Max Max Max Max Sum Sum Max Sum Max Sum Sum Max Sum Max Sum Sum Max Max Sum Sum Sum Sum Max
%IncMSC

Figure S7. Correlation of genomic features. (A) Correlation heatmap showing the individual correlations of each of the features (top) and legend representing which feature is represented (bottom). Scatterplot showing the predicted loop fold-change vs actual loop fold-change for the testing dataset for **(B)** CTCF loops, **(C)** non-CTCF loops, and **(D)** all loops with random forest regression. (Gray = static loops, teal = gained loops, maroon = lost loops, R^2 calculated for all loops included in the testing dataset). **(E)** Individual feature absolute coefficients from the linear model including all features, ordered by decreasing absolute coefficients (top). Legend representing which feature is represented in the barplots (middle). Percent Included Mean Squared Error (%IncMSE) for all of the features included in the random forest model, in the same order as the features from the linear model (bottom).

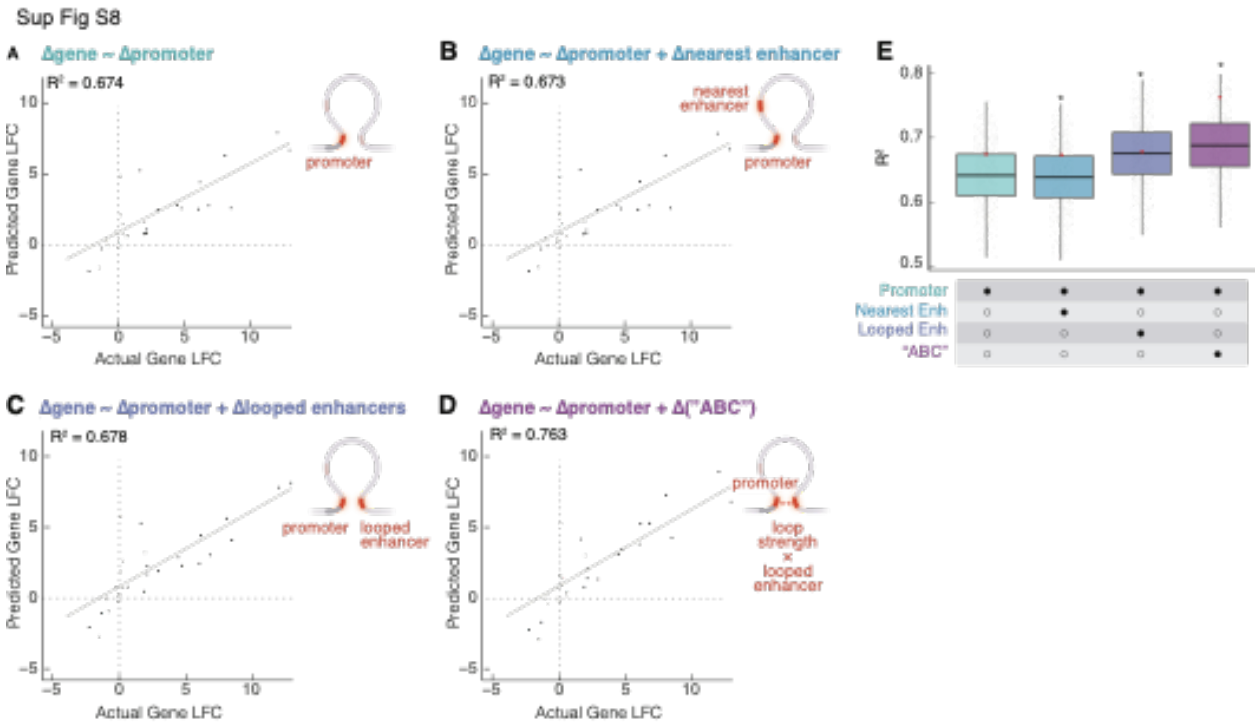

Figure S8. Changes in gene expression at differential loops are explained by combined proximal and distal enhancer activity and loop strength. Scatter plots showing predicted gene-fold change vs actual gene fold-change for genes that are at the anchors of differential loops based on one permutation of **(A)** promoter H3K27 ac LFC alone, **(B)** promoter H3K27ac LFC and the nearest enhancer to the promoter's FC, **(C)** promoter H3K27ac FC and distal looped H3K27ac, and **(D)** promoter H3K27ac LFC and the LFC of the product of distal looped H3K27ac and loop strength (red = differential gene, gray = static gene). **(E)** R^2 for each model calculated based on 1000 permutations of splitting data into training and testing sets. Wilcoxon rank sum test was performed to compare each group to the promoter only model, asterisk represents $p < 0.05$. Red dots represent the single permutation from A-D.